TECHNISCHE MECHANIK, 32, 2-5, (2012), 425 - 434
submitted: October 26, 2011

Variable Local Moduli of Elasticity as Inputs to FEM-based Models of Beams made from Glued Laminated Timber

L. Melzerová, P. Kuklík, M. Šejnoha

The present paper is concerned with the formulation of advanced FEM based models of beams made from glued timber segments. These models account for variable elastic moduli in individual segments and their analysis is based on the application of LHS method. All results from probabilistic calculations are compared with experimental measurements conducted on twenty beams as well as with the FEM results derived for the same beams assuming deterministic analysis with piecewise constant moduli in individual segments. The main contribution of enhanced probabilistic models is seen primarily in the ability to provide cost effective designs of long-span glued timber structures.

1 Introduction

The present contribution builds upon an extensive experimental program examining the behavior of glued laminated timber beams. Twenty beams were tested at the Department of Steel and Timber Structures of the Faculty of Civil Engineering in Prague. Two types of experiments were conducted. First, non-destructive measurements were performed to measure the elastic moduli of timber in the fiber direction at 1448 locations while monitoring the current state of moisture. The second type of experiments, performed on twenty beams, corresponds to destructive four-point bending tests with the option to measure various parameters with principal attention accorded to deflection at the center of beams. This parameter is not only decisive from the engineering practice point of view, since the limit deflection is typically reached prior to exceeding the bearing capacity, but it also serves as the most objective measure of the behavior of strongly heterogeneous materials such as the analyzed glued laminated timber. Both types of experiments will be reviewed in the first part of this text.
The second part is then concerned with the finite element (FE) simulation of these experiments including the introduction of material uncertainty through a variable Young's modulus. The first series of calculations assumes constant moduli assigned to individual segments as averages of values measured for a given segment. The numerical results show a relatively good agreement of this deterministic approach with experiments. The next part of the paper then deals with probabilistic simulations of the same beams assigning to each segment of the beam Young's modulus with a given probability of distribution. Individual samples (realizations), eventually providing the probability density function or the distribution function of the maximal deflection, are generated using the Latin Hypercube Sampling (LHS) method.
The results from the three approaches – experiment, deterministic and probabilistic numerical analyses – are compared next for two levels of the applied load. The first reference load level was accommodated by all twenty experimentally examined beams with no failure. For this load level the deterministic analysis shows a very good agreement with experiments. Probabilistic simulations with variable moduli provide even better predictions. The second load level corresponds to the maximal load which when exceeded leads to failure destruction of the beam. The results show a similar trend with improved predictive power of probabilistic simulations. Nevertheless, the agreement with experimental results is less satisfactory, which can be attributed to the initiation of cracks prior to the catastrophic failure, which is not reflected by purely elastic FEM simulations. The paper closes by presenting a general methodology for the preparation of the FEM models of the glued timber beams with variable moduli of elasticity and application of the methodology in practice for exceptional long-span structures.

2 Experiments

As already mentioned in the introductory part, the experimental program assumed two types of experiments to examine the behavior of glued laminated timber. An illustrative example of a glued laminated timber beam appears in Figure 1. In general, such a beam consists of an arbitrary number of segments glued together over their entire area to form a layered structure. As seen in Figure 2 the present example assumed eight layers (lamellas).

Our previous work was also concerned with the FEM modeling of the gluing effect by introducing an additional layer of glue along the longitudinal joints of individual segments thus allowing for the evolution of progressive delamination. However, based on experimental observations, suggesting no damage within these joints due to delamination when exceeding the overall bearing capacity, this approach was not pursued any further and a perfect bonding is assumed in the present study. The onset of cracking was detected in the locations of various flaws such as knots and not within the glued joints. No interface slip was also confirmed by the resulting deflections. Therefore, our attention has been shifted to the examination of the random nature of such structures as described in the next sections.

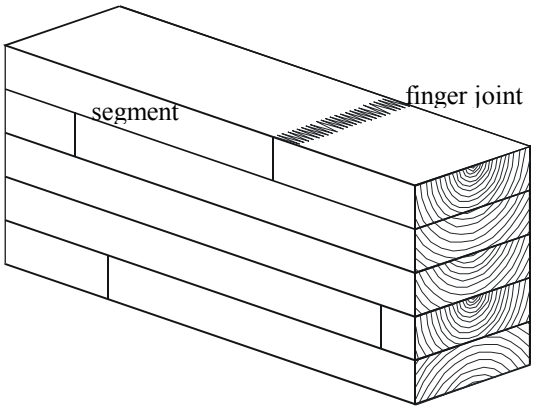

Figure 1. Illustration of glued laminated timber

Figure 2. Cross-section of tested beam

Individual layers in the laminated beam are usually not compact but are subdivided into segments each having a random length. This arises from cutting out sections of lamellas containing large knots and other possible flaws to improve the overall quality of the beam. This creates sections which are shorter than the beam length. These segments are placed randomly within the beam and connected by finger joints, Figure 1. A random distribution of segments of timber of a different quality results in a high variance of material properties within the beam and their discontinuous character. One should also realize that wood experiences a considerable variability in its properties even within individual segments. This clearly demonstrates the complexity of the accurate modeling of glued timber structures often avoided by accepting certain simplifications leading, however, to cost ineffective designs. On the contrary, it opens the way to probabilistic modeling as an obvious alternative, which is expected to offer the improved designs of all structures made from glued laminated timber and particularly of extreme long-span structures.

Figure 3. Pilodyn 6 J

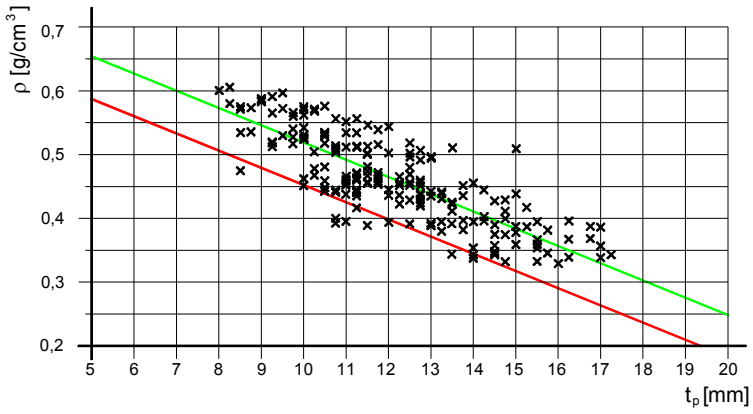

Figure 4. Variation of timber density as a function of indentation depth

As evident from Figure 1 the segment is referred to as a part of lamella between two finger joints or between the joint and the beam face. In sporadic cases a single segment spans the entire lamella. The overall number of segments in all twenty beams amounts to 362. The modulus of elasticity was measured for every segment at four different points which resulted in 1448 measured values. If limiting our attention to the verification of a general methodology for the formulation of FEM based computational models, this number appears sufficient although it might be necessary to be increaseed if one is interested in a particular structure.
The Pilodyn 6J measuring device, see Figure 3, is adopted to determine elastic moduli experimentally. The device shoots the indenter tip into the wood with a given energy and measures the indentation depth with 0.1 mm accuracy while simultaneously controlling the wood moisture. The measured depth, possibly adjusted to 12% of moisture, is then linked to a local wood density as plotted in Figure 4. The required local modulus of elasticity in the fiber direction (E in MPa) can be determined indirectly either from the wood density or from the measured indentation depth (t_p in millimeters, adjusted to 12% of moisture) according to

$$E = -564.1 * t_p + 19367 \tag{1}$$

The experimentally derived values were checked first approximately (globally) by comparing an expected maximal deflection with that provided by an independent bending test, and second more rigorously by measuring local strains with the help of strain gauges applied at several locations of high stresses developed during the bending test. Given an approximate value of the local stress calculated for a homogeneous body the modulus of elasticity can then be determined from Hook's law and compared with the corresponding measured value.

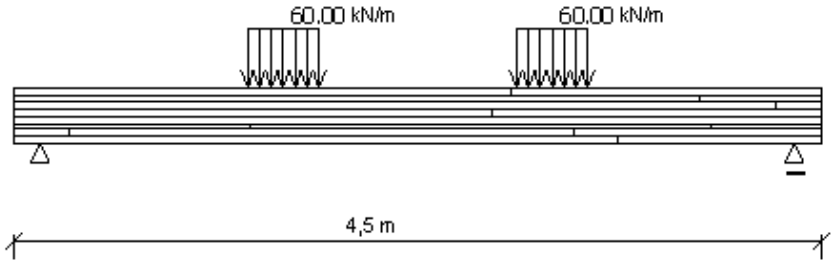

Figure 5. Sketch of four-point bending test

Figure 6. Beam loading

Figure 7. Stabilization against overturning (lateral buckling)

The four point bending test is schematically shown in Figure 5 and documented by photographs in Figure 6. The center beam deflection was measured by a displacement sensor corrected for support compression by installing two other sensors at their vicinity. The loading was supplied by two forces at one third of the beam span through two cylinders of a loading press, see Figure 7. This figure also displays provisions applied to secure the beam against lateral buckling. A 40 cm long steel plate was placed below each force to allow for the introduction of a distributed loading as also assumed in the numerical tests. Both forces were gradually increased up to complete failure with a loading step equal to 4 kN. Each load step followed by a hold period to collect the data from all measuring sensors. The failure load for individual beams experienced a considerable scatter from 30 to 60 kN.

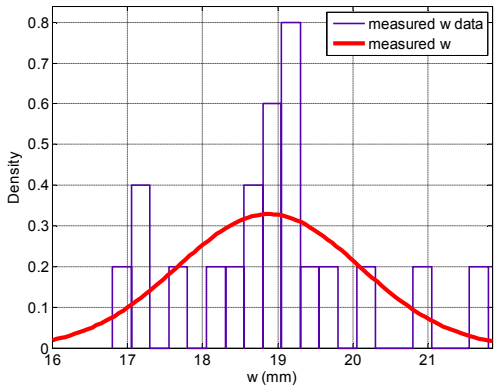

Figure 8. Gaussian probability density function of measured displacements

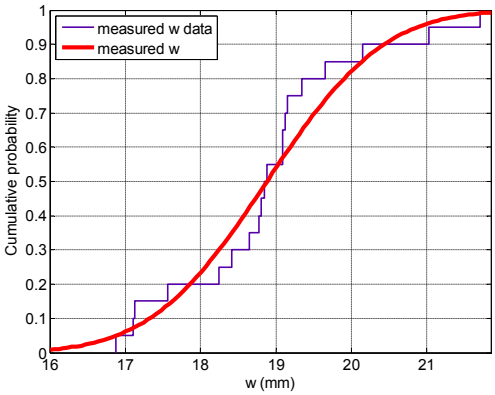

Figure 9. Distribution function of measured displacements

The measured deflections, adopted in this study for the sake of comparison, were statistically evaluated for two different load levels. The results for the first load level of 24 kN for each force corresponding to 60kN/m uniformly distributed load are plotted in Figures 8 and 9. Figure 8 provides the Gaussian probability density function estimated from 20 measurements. Figure 9 then shows the corresponding distribution function.

3 Deterministic Modeling using FEM

The resulting elastic moduli delivered by experimental measurements have already been evaluated in the previous section assuming all 1448 measured values. Deterministic FEM based modeling discussed in this section requires, however, an averaging of these values over individual segments yielding a new set of data, which can also be statistically evaluated. The results appear in Figures 10 and 11 (solid line in red color corresponds to all 1448 measurements) suggesting higher uncertainty when taking into account all measurements and possible misrepresentation of input data associated with the used local averages of Young's moduli.

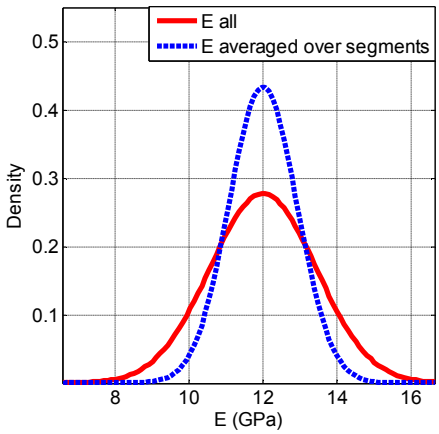

Figure 10. Comparison of probability density functions of Young's modulus derived from all 1448 measured data and from values averaged over individual segments

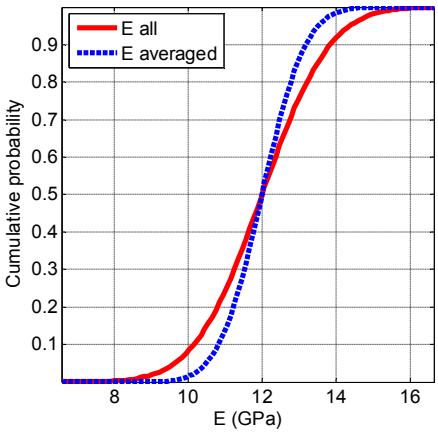

Figure 11. Comparison of distribution functions of Young's modulus derived from all 1448 measured data and from values averaged over individual segments

The results presented in this and the subsequent sections are derived on the basis of several simplifying assumptions including two-dimensional (2D) plane stress analysis and piecewise isotropic material. It has been found that errors associated with these simplifications when compared to the predictions provided by a three-dimensional analysis while also accounting for a material orthotropy are rather negligible and are of the order of magnitude smaller in comparison with measurement errors arising in experiments. The adopted computational model is plotted in Figure 12 also showing relatively fine finite element mesh. To further appreciate a structural heterogeneity due to different elastic moduli in individual segments as well as structural variability of individual beams we also show a concrete pattern of segments for three selected beams. Figure 13 corresponds to an average beam rendering the maximal deflection close to the average value calculated from all twenty specimens. Figure 14 illustrates an example of a beam having a large number of segments with low moduli of elasticity which are not even arranged in favor of the static response thus yielding a large deflection. Contrary to that, Figure 15 displays an example of a majority of segments having the above average value of Young's modulus, which are randomly arranged such as to provide one of the stiffest response. Notice that segments with lower moduli of elasticity are found in the vicinity of the neutral axes, whilst segments with higher moduli are located in outer lamellas. Also recall that the presented deflections correspond to a uniform load of 60 kN/m.

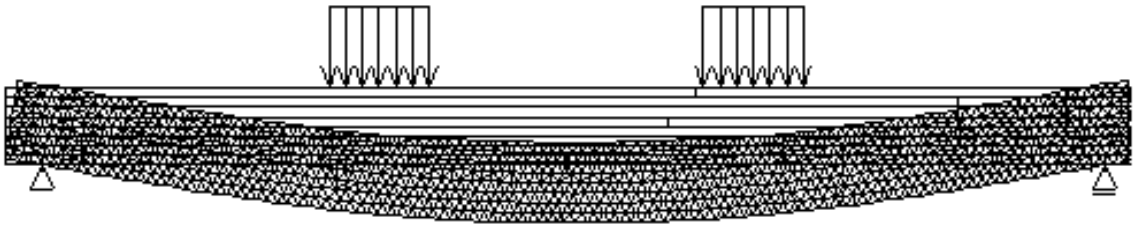

Figure 12. Illustrative example of FEM model

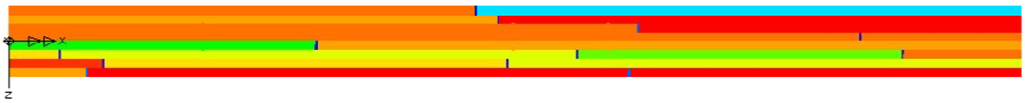

Figure 13. Distribution of averages of Young's moduli within the beam with average deflection of 18.88 mm

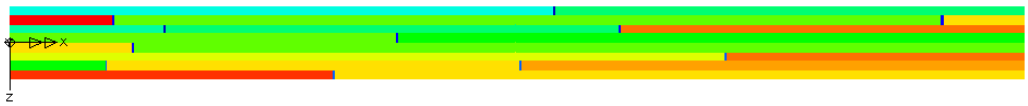

Figure 14. Distribution of averages of Young's moduli within the beam with large deflection of 21.7 mm

Figure 15. Distribution of averages of Young's moduli within the beam with small deflection of 16.87 mm

4 Probabilistic Modeling using FEM

The advanced FEM models employ probabilistic simulations performed in the framework of the LHS method. In the light of this, to each segment we assigned a Young's modulus with a corresponding probability density function. In all cases the Gaussian distribution with the given mean and standard deviation is assumed as seen in Figure 16. The associated distribution function is then utilized to generate individual samples. In the present study the distribution function was split into 100 intervals to randomly select a single value ${}^{k}E$ as schematically shown in Figure 17. This result is in accord with the LHS method based on 100 strata. The resulting map of realizations, see Table 1, is constructed such as to comply with a statistical independence of elastic moduli from segment to segment. Note that the selection of lamellas to form a beam is conducted in a totally random manner. Figure 18 shows a variation of maximal deflections from 100 samples derived for a single beam with a given

pattern of segments. These results can be statistically evaluated and fitted to the selected probability density function as illustrated in Figure 19 with the corresponding plot of the distribution function in Figure 20 for the Gaussian distribution. The log-normal analog is presented in Figures 21 and 22, respectively. Owing to a negligible difference between the Gaussian and log-normal fits of the discrete ensemble of maximal deflections, the Gaussian distribution will be referred to in all subsequent discussions.

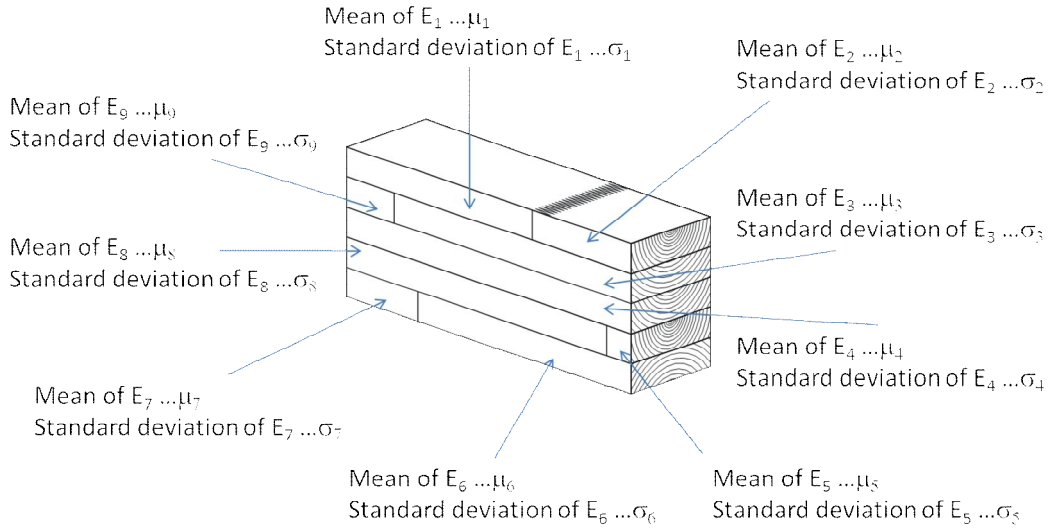

Figure 16. Illustration of the input data used in the LHS method

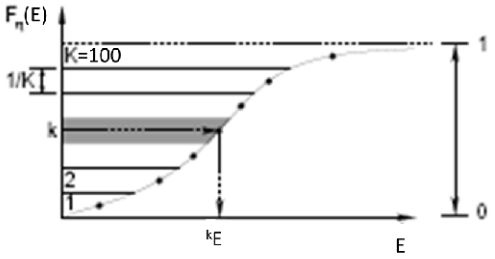

Figure 17. Principle of selecting the k-th sample in the LHS method

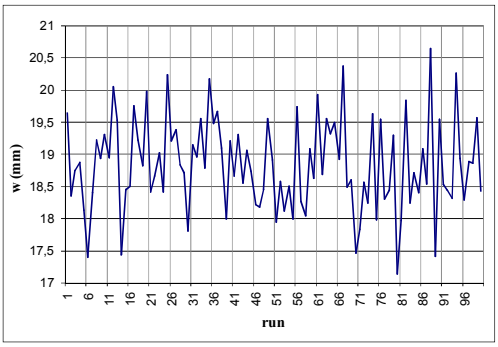

Figure 18. Resulting maximal deflections for a single beam from one hundred realizations

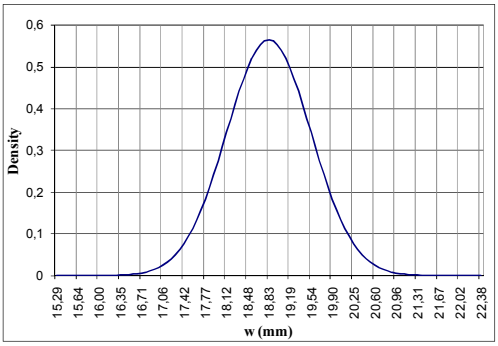

Figure 19. Example of the Gaussian probability density function of deflection for the selected beam

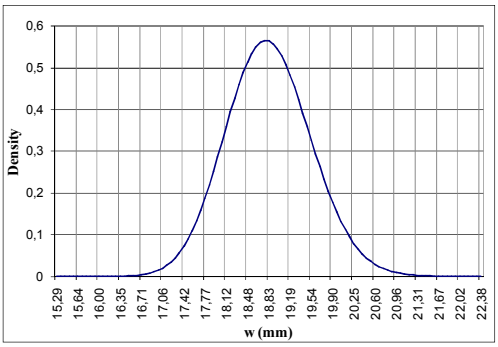

Figure 21. Example of the Log-normal probability density function of deflection for the selected beam

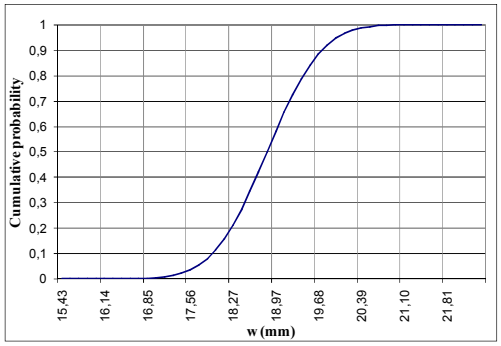

Figure 20. Example of the Gaussian distribution function of deflection for the selected beam

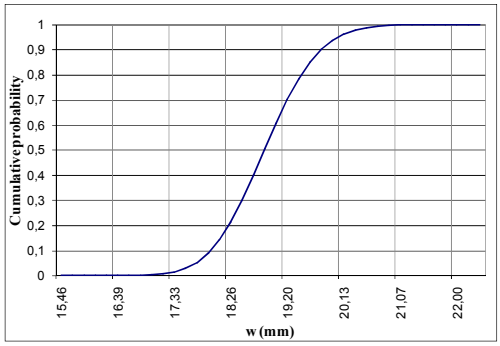

Figure 22. Example of the Log-normal distribution function of deflection for the selected beam

Segment 1	$^{5}E_{1}$	$^{90}E_{1}$	$^{16}E_{1}$	…	$^{4}E_{1}$
Segment 2	$^{11}E_{2}$	$^{7}E_{2}$	$^{3}E_{2}$	…	$^{92}E_{2}$
……				…	
Segment 18	$^{85}E_{18}$	$^{1}E_{18}$	$^{5}E_{18}$	…	$^{10}E_{18}$
	Beam for run 1	Beam for run 2	Beam for run 3		Beam for run 100

Table 1. Example of creating individual realizations using the LHS method for a beam with 18 segments and 100 strata

5 Comparing Results from FEM Simulations and Experiments and their Evaluations

This section compares the results provided by the individual methods. The results derived from the deterministic FEM modeling for the uniformly distributed load level equal to 60 kN/m are compared with the corresponding experimental values in Figure 23 for all twenty specimens. It is evident that the resulting differences experience both positive and negative sign not showing a unique pattern. This is in contradiction to the plot in Figure 24 presented for a maximal loading pertinent to each beam where the FEM results are consistently below the measured values. This is what one would expect, since in reality the beams may an witness evolution of local damage even prior to reaching an ultimate load not addressed by the elastic FEM analysis. From the absolute value point of view the differences are, however, in the same range as in the case of elastic loading (Figure 23), note two different scales of vertical abscissa in Figures 23 and 24.

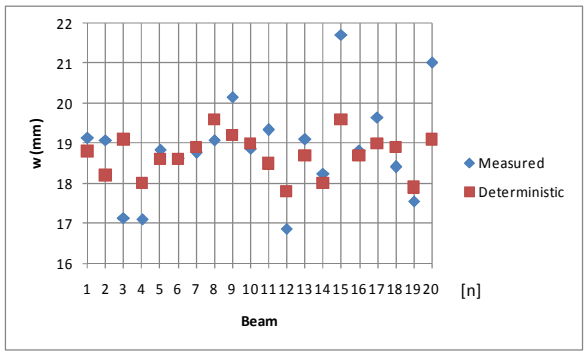

Figure 23. Comparison of measured and numerically derived deflection using deterministic FEM model applied to 20 beams each loaded by 60 (kN/m)

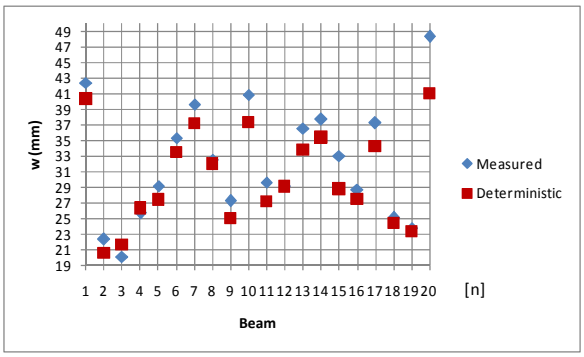

Figure 24. Comparison of measured and numerically derived deflection using deterministic FEM model applied to 20 beams loaded by their maximal loading

Henceforth, attention will be dedicated to the results provided by probabilistic simulations. To compare individual approaches (experiment, deterministic and probabilistic modeling) a single value given by the averages obtained from 100 samples, see also Figures 19 to 22, will be adopted. This appears in Table 2 suggesting in such a case no need for more advanced and computationally exhausted probabilistic simulations. It might be, however, expected that a better agreement with experimental results will be obtained with improved probabilistic data of input parameters conditioned by considerably more measurements in individual segments (recall that only four measurements are presently available for each segment). Probability of not exceeding a certain limit deflection is even more important than a simple mean, although not examined, which might provide further insight in the behavior of such structures.

	w (mm)	**Percent of measured**
Measured	19.15	100
Discrete FEM	18.8	98.17
LHS	18.83	98.34

Table 2. Comparison of measured and numerically derived deflections for the selected beam

Figures 25 and 26 then compare the probability density functions and the distribution functions, respectively, estimated from the results provided by all 20 specimens (in case of probabilistic modeling we assumed the ensemble of 20 averages of maximal deflections). The corresponding statistics used to construct these functions are stored in Table 3. For the computational results the probability density function is re-plotted in Figure 27. The variations of maximal deflections in Figure 23 are finally re-plotted in Figure 28 showing also the comparison with the averages delivered by the probabilistic analysis. Clearly, when comparing only averages the difference between deterministic and probabilistic modeling is almost negligible. Recall, however, that above each mean value one should image a particular distribution, $f_{W,n}(w)$, as also schematically shown in Figure 28.

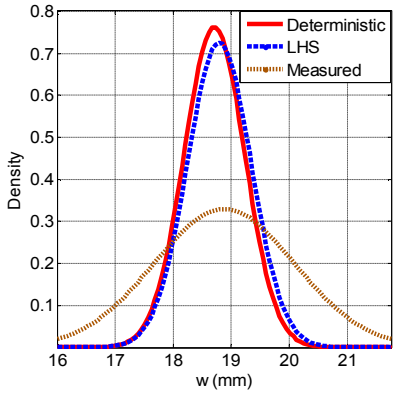

Figure 25. Comparison of Gaussian probability density functions of both measured and calculated deflections from the ensemble provided by all 20 beams

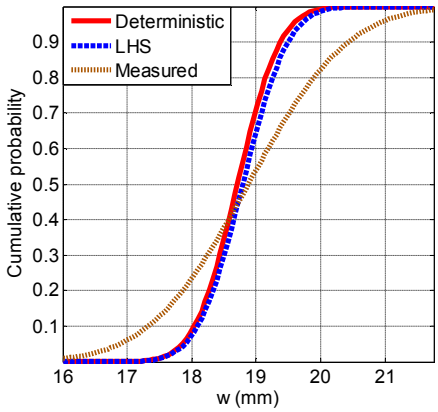

Figure 26. Comparison of distribution functions of both measured and calculated deflections from the ensemble provided by all 20 beams

	μ	**σ**
Measured	18.88	1.213
Deterministic FEM	18.71	0.523
Probabilistic FEM (LHS)	18.79	0.550

Table 3. Comparison of statistical data evaluated from the ensemble of deflections provided by all 20 beams

This alows us to estimate the probability of exceeding a certain level of the assumed allowable deflection of the beam $\overline{w}$ as

$$P(w > \overline{w}) = 1 - \frac{1}{N} \sum_{n=1}^{N} F_{W,n}(w), \tag{2}$$

where N is the number of beams and $F_{W,n}$ is the corresponding distribution function of the deflection of the n-th beam.

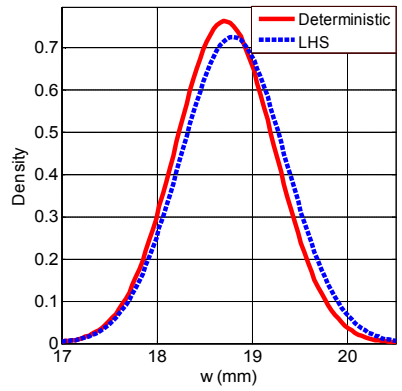

Figure 27. Comparison of Gaussian probability density functions of calculated deflections from the ensemble provided by all 20 beams

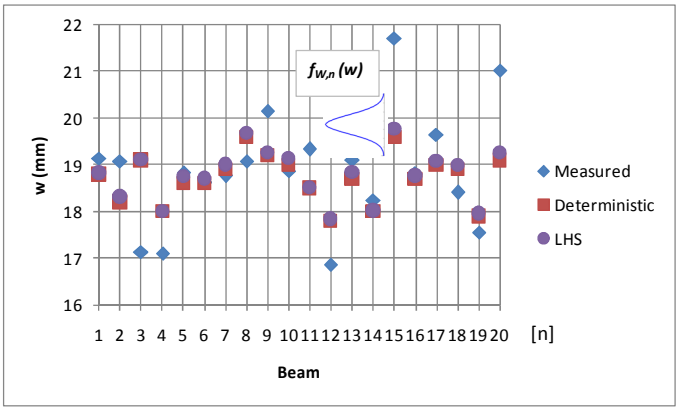

Figure 28. Comparison of measured and calculated deflections (the circles show averages from 100 realizations obtained for individual beams)

6 Conclusions

The presented results demonstrate that a certain improvement in the prediction of the response of glued timber beams can be achieved by extending the deterministic modeling to allow for a variability of input parameters in the framework of probabilistic simulation. However, the degree of improvement strongly depends on the quality of input parameters being in turn dependent on the number of available laboratory measurements. The actual computational methodology is nevertheless independent of such data. It is not surprising that the results from the two approaches are rather similar since we compared on the basis of averages only. Information provided by the stochastic analysis is, however, significantly broader, recall Equation (2).

The proposed technology of determining deflection and stress or strain distributions assumes a synergy of experimental measurements of local moduli and FEM based analysis of a given structure with random material data. Although verified on a relatively small set of twenty beams, its practical applicability is expected in the design of unique nonstandard glued laminated timber structures.

Acknowledgement

This outcome has been achieved with the financial support of the Ministry of Education, Youth and Sports of the Czech Republic, project No. 1M0579, within activities of the CIDEAS research centre.

References

Melzerová, L.; Kuklík, P.: Statistical Research of Mechanical Properties of Glued Laminated Timber Beams. *Metallurgy,* 49, (2010), 376-380.

Melzerová, L.; Kuklík, P.: Beams from the Glued Laminated Timber Experiment versus FEM Model. *World Academy of Science, Engineering and Technology*, 55, (2009), 262-266.

Vořechovský, M.: *Stochastic computational mechanics of quasibrittle structures*, Ph.D. thesis, Brno University of Technology, (2007).

Šejnoha, M; Šejnoha, J; Kalosková , M.; Novák, J; Zeman, J.: Stochastic analysis of failure of earth structures. *Probabilistic Engineering Mechanics*, 22(2), 206–218, (2007).

Address: Ing. Lenka Melzerová, Ph.D., Doc. Ing. Petr Kuklík, CSc., Prof. Ing. Michal Šejnoha, Ph.D, DSc., Faculty of Civil Engineering, Czech Technical University in Prague, Thákurova 7, 166 29 Praha 6, Czech Republic, email: melzerov@fsv.cvut.cz ; kuklik@fsv.cvut.cz ; sejnom@fsv.cvut.cz